that χ_S^L is also a lower bound for the adiabatic susceptibility which may be obtained from Eq. (32) by making the entropy constant (the constant entropy does not mean, in general, the constant population).

[5]N. Bloembergen and P. Lallemand, Phys. Rev. Letters 16, 8 (1966); S. Kielich, Acta Phys. Polon. 30, 683 (1966); R. W. Hellwarth, Proceedings International School of Physics "Enrico Fermi," Varenna, Italy, 1967 (unpublished); M. Takatsuji, Phys. Rev. 165, 171 (1968); J. Hanus, *ibid.* 178, 420 (1969).

[6]M. Takatsuji, Phys. Rev. 155, 980 (1967).

[7]M. Takatsuji (unpublished).

PHYSICAL REVIEW B VOLUME 2, NUMBER 2 15 JULY 1970

Effective Mass and Spin Splitting in $Hg_{1-x}Cd_xTe$

G. A. Antcliffe

Texas Instruments Incorporated, Dallas, Texas 75222

(Received 15 January 1970)

Shubnikov-de Haas measurements have been performed on single-crystal n-type $Hg_{1-x}Cd_xTe$ ($x = 0.204$) alloys with carrier concentration from 2×10^{15} to 1×10^{16} cm^{-3}. Comparison of the electron effective mass as a function of Fermi energy with $\vec{k}\cdot\vec{p}$ theory yields the following band parameters: band-edge mass $m_0^* = 5.60\pm0.25\times10^{-3}\,m_0$, interband matrix element $E_p = 17\pm1.4$ eV, and direct energy gap (at $k=0$) $E_g = 0.0635\pm0.008$ eV. We also observed spin splitting of the $N=1$, 2, and 3 Landau levels, from which the electron g factor was determined as a function of energy between 8 and 23 meV from the conduction band edge, with $g = 164\pm16$ at the band edge.

I. INTRODUCTION

The $Hg_{1-x}Cd_xTe$ alloy system is of considerable interest from several viewpoints. $Hg_{1-x}Cd_xTe$ at $X=0$ is a semimetal which exhibits a semiconductor-semimetal transition at $x\simeq0.18$, which is not yet completely understood.[1] As x is increased further, the energy gap at $k=0$ between a Γ_6 conduction band and the Γ_8 valence bands increases to about 0.10 eV at $x\simeq0.21$[2] and around this composition sensitive 8–14-μ photoconductors have been reported.[3] For an excellent summary of earlier work and for a discussion of the variation in band structure through the $Hg_{1-x}Cd_xTe$ system, we refer the reader to two excellent reviews[4] and references cited therein. We will be concerned in this paper only with one alloy composition — $Hg_{0.796}Cd_{0.204}Te$, where the conduction band has Γ_6 character. While there is agreement that this Γ_6 band is nonparabolic and should be described adequately by Kane's $\vec{k}\cdot\vec{p}$ theory,[4–6] developed for the Γ_6 band of InSb,[7] there is, at present, no systematic confirmation of this near the band edge for the semiconducting alloys ($x>0.18$). Interest has generally centered on investigations of the physical properties as functions of Cd concentration, with detailed measurements being rare due to the difficulty in attaining homogeneity in this system.[4] For example, the recent helicon propagation results[8] in low carrier concentration $Hg_{1-x}Cd_xTe$ still do not allow complete characterization of the Γ_6 band. We present in this paper the first detailed measurements on single-crystal low-concentration n-type $Hg_{1-x}Cd_xTe$ ($x=0.204$) using the Shubnikov–de Haas effect at liquid-helium temperatures. The experiments are aimed specifically at a determination of the Γ_6-band parameters, at *one* alloy composition, where the energy gap is close to 0.064 eV at 4.2 °K. The single-crystal alloys used in the present study had electron concentrations between 2×10^{15} cm^{-3} and 1×10^{16} cm^{-3} and electron mobilities greater than 2×10^5 cm^2/V sec at helium temperatures. We have determined the electron effective mass over this carrier concentration range and observed spin splitting of the lower quantum number Landau levels, which has allowed us to determine the energy dependence of the electron g factor. Limits have also been placed on the sphericity of the Fermi surface from the angular dependence of the Shubnikov–de Haas period.

We describe in Sec. II the experimental details together with a discussion of criteria which must be considered to ensure reliable Shubnikov–de Haas data. The results are presented in Sec. III together with a comparison with Kane's $\vec{k}\cdot\vec{p}$ theory. The relevant formulas from the theory are well known and summarized in the Appendix.

II. EXPERIMENTAL DETAILS

The single-crystal $Hg_{1-x}Cd_xTe$ alloys from which the experimental samples were cut were grown

by a solid-state recrystallization technique.[9] The generally unoriented single-crystal samples were about $10\times2\times0.5$ mm, and contacts were made by indium soldering after etching in bromine-methanol. Several samples were oriented by backreflection Laue photographs. However, since no dependence on the magnetic field orientation was observed in the period of the oscillatory magnetoresistance, most measurements were made on unoriented single-crystal samples. Generally the data reported below were taken with the magnetic field H perpendicular to the direction of current flow. The alloys used were cut from ingots randomly doped by unknown trace impurities such that the electron concentrations were in the range 2×10^{15} to 1×10^{16} cm^{-3}. The mole fraction $x=0.204$ was very homogeneous throughout the whole source ingot from which our samples were cut, being about ±0.003 mole fraction over 10 mm as determined from relative spectral response and Cd^{115} radioactive tracer analyses.[3]

The annealing procedure involved in the crystal growth process was progressively optimized so that finally electron mobilities μ_n better than 2×10^5 cm^2/V sec were attained for the lower-concentration samples and greater than 1×10^5 cm^2/V sec for carrier densities up to 10^{16} cm^{-3}.

The oscillatory signals were detected by a sensitive derivative recording technique[10] in which the sample was mounted between two small coils providing an ac modulation field. Magnetic fields up to 20 kG were provided by a superconducting solenoid in which the samples could be rotated by a gear arrangement extending into the helium cryostat. Bath temperature was monitored by a Texas Instruments precision pressure gauge.

We now discuss briefly the quality of the $Hg_{1-x}Cd_xTe$ used in the present investigation. As mentioned above, the homogeneity problem is particularly severe because of the large separation of the solidus and liquidus lines.[4] While the solid-state recrystallization technique gives much greater uniformity in mole fraction x than does a Bridgman-type technique, one must rely on impurity diffusion below the melting point to obtain homogeneity in carrier concentration. We have made use of the Shubnikov–de Haas oscillations to gauge the variation in carrier concentration along our samples by evaporating a series of 10-mil-diam indium dots along the sample and recording the periodicity of the oscillations between successive pairs of dots. The oscillatory period denoted by $\Delta(1/H)$ is directly related to the carrier concentration n for a spherical Fermi surface since in this case $\Delta(1/H)=(2e/\hbar c)(3\pi^2n)^{-2/3}$. This relation is valid for $Hg_{0.796}Cd_{0.204}Te$ since we find that the Fermi surface is spherical to within $\pm2\%$ (Sec. III). The resolution of this technique is limited by the requirement that a measurable voltage must appear between adjacent dots. A spacing of 20 mil was used, but we are of the opinion that this could be reduced considerably without degrading the oscillatory signal too badly. For the best samples, we observed less than a 10% variation in n over a distance of 0.5 mm. Inhomogeneity can also affect the envelope of the oscillations as shown in Fig. 1. From the regions labeled A and C, the oscillatory magnetoresistance appears as expected, increasing in amplitude with increasing magnetic field with periodicity in $1/H$. However, region B is sufficiently inhomogeneous in n (possible also in x) to introduce a second oscillatory component. Because of level broadening, the oscillatory amplitude of B has been reduced. Useful data were obtained only from regions such as A and C, but such areas could be located on all specimens between at least one pair of indium dots. This technique provides a much more sensitive probe than a resistivity profile and has indicated that there is still microinhomogeneity on a scale smaller than 10 mil when the carrier concentration is in the low 10^{15} range. This may be due to partial compensation at these electron concentrations.

In many instances, particularly in the early phases of this investigation, we were unable to obtain a reliable determination of the electron

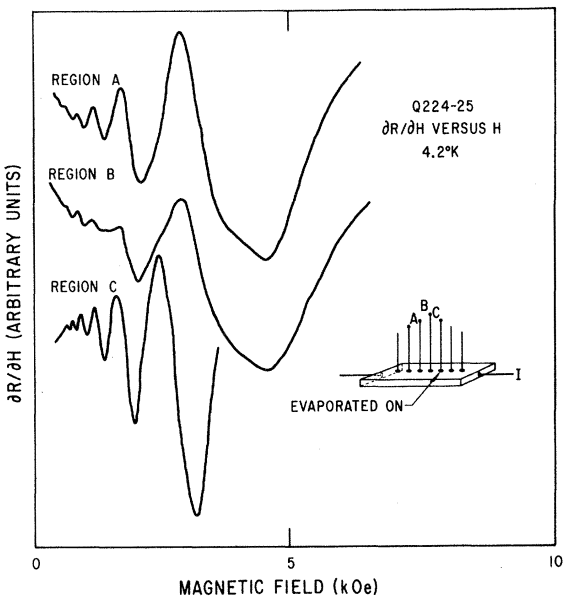

FIG. 1. First derivative of sample resistance versus magnetic field showing the Shubnikov–de Hass oscillations from three adjacent pairs of contacts along sample Q224-25. From regions such as B, no reliable data can be obtained. The structure in the last derivative minimum in the A trace is a spin-splitting effect (see text).

effective mass from the temperature dependence of the Shubnikov–de Haas amplitude. This is a standard technique of mass measurement since the ratio of the oscillatory amplitude at two temperatures T_1 and T_2 ($T_2 < T_1$) is given by[11]

$$\frac{A(T_2)}{A(T_1)} = \frac{T_2 \sinh U_1}{T_1 \sinh U_2}, \quad U_i = \frac{2\pi^2 k T_i}{\hbar\omega_c}, \quad \omega_c = \frac{eH}{m^* c}.$$

Often we observed that the envelope of good oscillatory data (e.g., region A or C above) did not increase uniformly with decreasing temperature. We are of the opinion that this was due to the presence of inhomogeneity, and such samples were discarded. We also observed an additional effect which strongly perturbed the mass determination, particularly in the low-carrier-concentration samples. The values of m^* derived from progressively higher magnetic field oscillations often increased toward a high-field-limiting value. This was due to heating of the electron system by the applied dc bias which caused the electron temperature to increase above the lattice temperature. The electric field across the sample when such results were obtained was about 20 mV/cm. Since the magnetic field "cools" the electron system, we expect to approach the correct value of m^* at the higher magnetic fields; by reducing the dc bias we verified that this was indeed the case.

Finally, we wish to make some comments concerning the magnitude of the energy gap at $k = 0$ in $Hg_{0.796}Cd_{0.204}Te$. The structure of the valence bands near $k = 0$ in the semiconducting alloys is not completely understood, so there exists some doubt concerning the detailed variation of E_g near the extrema. For $x = 0.204$, it has been found in our laboratories that the 50% relative spectral response threshold wavelength for photoconductivity in low-concentration samples is $\lambda = 13.7 \pm 0.5\ \mu$ at 77 °K,[3] where the quoted error includes data from many ingots. We have not been able to measure the threshold for the more heavily doped samples used in the present work, but there is no reason to expect the threshold to be outside the limits given above since the conditions of growth were identical. At 4.2 °K, the threshold wavelength is found to increase by a factor of 1.37, implying a direct band gap $E_g^p = 0.0665 \pm 0.002$ eV. This increase may be compared with that predicted by several formulas available in the literature which relate E_g to x and T. For $x = 0.204$, we have

$$E_g = 0.090 + 2.96 \times 10^{-4} T \text{ eV}, \quad \text{(Ref. 8)}$$

$$E_g = 0.074 + 3.01 \times 10^{-4} T \text{ eV}, \quad \text{(Ref. 12)}$$

$$E_g = 0.050 + 3.30 \times 10^{-4} T \text{ eV}, \quad \text{(Ref. 13)}$$

from which $E_g(77)/E_g(4.2)$ is 0.114/0.091 = 1.26, 0.097/0.075 = 1.29, and 0.075/0.051 = 1.48, respectively. Note the rather wide spread in the magnitude of the energy gap predicted by each formula. This discrepancy apparently stems from variations in the determination of mole fraction x in the alloys grown by different techniques in different laboratories. This problem has been discussed elsewhere[4,8] and we will not consider it further. However, we are confident that the true energy gap of our $Hg_{0.796}Cd_{0.204}Te$ alloys will not differ from E_g^p by more than the Fermi energy in the photoconductive samples, which is $\simeq 4$ meV (see Table I).

TABLE I. Electron effective mass ratio m^*/m_0 and spin splitting δ_{obs} for six samples of the alloy $Hg_{0.796}Cd_{0.204}Te$. Also listed are the periodicit, $\Delta(1/H)$, carrier concentration n, and the g values. The Fermi-energy values E_F were derived from the measured masses using Eq. (A3).

Sample	$\Delta(1/H)$ (10^{-4} Oe^{-1})	($n \times 10^{-15}$) cm^{-3}	(m^*/m_0) $\times 10^{-3}$	E_F(meV)	δ_{expt}	g
Q228-9	1.80	2.32	7.02	8.0	0.48	137
Q270-22	1.50	3.10	7.55	11.0	0.45	119
Q190-15	0.98	5.90	8.30	15.2	0.48	115
Q269-11	0.90	6.60	9.10	19.7	0.45	99
Q269-30	0.81	8.00	9.20	20.4	0.47	100
Q193-19	0.645	9.66	9.66	23.0	0.44	93

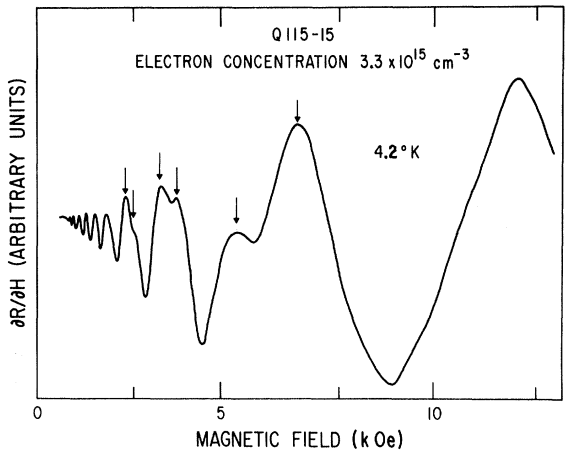

FIG. 2. Typical x-y recording of the oscillatory magnetoresistance showing spin splitting on last three derivative maxima (marked by ↓).

III. RESULTS AND DISCUSSION

Figure 2, which is reproduced directly from an x-y recorder plot, illustrates the strong oscillatory signal obtained from all samples. The low-field oscillations could be recorded with a gain of 10× over that shown without degrading the signal-to-noise ratio appreciably.. Generally, the first derivative of the resistance with respect to H was

recorded. The threshold magnetic field H for the oscillations was very close to that predicted by $\mu_n H = 1\times10^8$ and from six to eight derivative peaks could be identified before spin splitting of the Landau levels began to be resolved. From the low-field data, we determined the periodicity in $1/H$ from the derivative extrema by plotting $1/H$ against integer numbers (Fig. 3). From the oscillatory envelope, one may also plot the magnetic fields, where $\partial R/\partial H = 0$, versus integer numbers to confirm that the structure at the Nth Landau level is, in fact, splitting on the $N = 1$, 2, and 3 levels. Even when the splitting is resolved, the periodicity in $1/H$ appears to be essentially constant. In Table I, we give the periodicity $\Delta(1/H)$ for six alloy samples together with the carrier concentration calculated from $\Delta(1/H) = 2e/\hbar c(3\pi^2 n)^{-2/3} = 3.18 \times 10^6/n^{2/3}(\mathrm{Oe}^{-1})$, a relation which is valid for a spherical Fermi surface. To ascertain the validity of this relation for $Hg_{0.796}Cd_{0.204}Te$, the angular dependence of $\Delta(1/H)$ was studied carefully in samples with electron densities to 1×10^{17} cm^{-3} by rotating the magnetic field in a $\{110\}$ plane. This plane contains both $\langle100\rangle$ and $\langle111\rangle$ directions along which distortion first appears at large k values in the Γ_6 band of InSb.[14] The oscillatory period was independent of the direction of the magnetic field to $\pm2\%$, implying a Fermi surface which is spherical to this accuracy. The above relation is therefore expected to be valid. The carrier concentration determined from the Hall coefficient was in satisfactory agreement with the value derived from the oscillatory period.

The monotonic magnetoresistance for a representative sample is shown in Fig. 4. The highest magnetic field maximum in ρ_{xx} is strong in the transverse geometry but barely detectable in the longitudinal orientation. A similar effect has been observed in HgTe[15] and attributed to a small probability of spin-flip scattering in the longitudinal orientation.[16] This maximum appears as the highest magnetic field derivative in a plot such as is given in Fig. 2 and is thus ascribed to the highest-energy spin state of the $N = 0$ level. The magnetic field H_0^+ at which the Fermi level crosses this level may be calculated from the electron g factor. We postpone the comparison, however, until we have discussed the relevant band parameters.

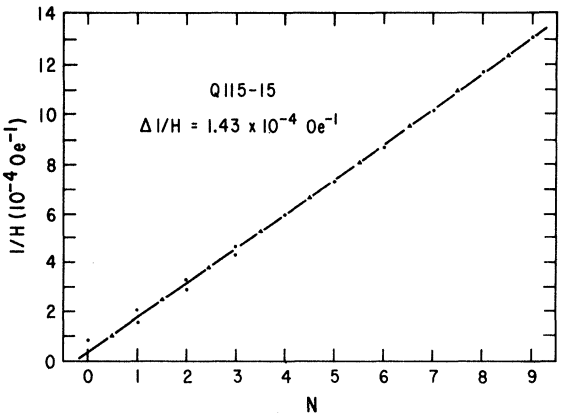

FIG. 3. Reciprocal of the magnetic field corresponding to derivative maxima (•) and minima (▲) versus integers. Spin splitting was observed on the last three maxima. The highest magnetic field point corresponds to the highest-energy spin state of the $N = 0$ Landau level.

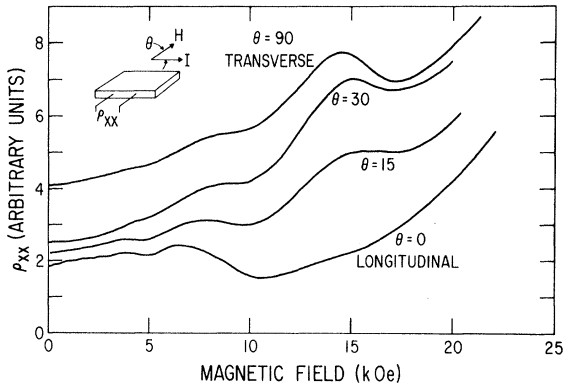

FIG. 4. Resistance measured between side contacts as a function of magnetic field strength. θ is the angle between the direction of current flow and the magnetic field and the traces have been displaced vertically for clarity.

In some of the more inhomogeneous samples, which, however, still showed excellent oscillatory signals, we observed that additional structure appeared as the magnetic field was rotated from the longitudinal to the transverse orientation. To elucidate this behavior, we recorded the oscillations in the Hall voltage and found them significantly out of phase with those in the magnetoresistance. It is well known[17] that sample inhomogeneity can mix ρ_{xx} and ρ_{xy}, the two components of the resistivity tensor, so one might expect to observe some ρ_{xy} character in ρ_{xx} when in the transverse geometry. The ρ_{xy} oscillations are weak except when the last two Landau levels are occupied, but it is just in this magnetic field range where the additional structure is observed. Therefore, we feel justified in ignoring such effects.

We have measured the electron effective mass by observing the change in oscillatory amplitude with temperature below 4.2 °K. Electron heating effects (Sec. II) were negligible. Generally, the amplitude of five oscillations (below the magnetic fields where spin splitting was observed) was determined at three temperatures between 4.2 and

1.5 °K and used to derive some 15 values of m^*/m_0, which were averaged to obtain the values given in Table I. This procedure is allowable since the amplitude envelope at low magnetic fields, where several levels are occupied, should yield values of m^*/m_0 which are independent of magnetic field. We used oscillations corresponding to $N > 3$ and $N > 6$ for the low- and high-concentration samples, respectively. We also give in Table I the Fermi energy derived from the measured masses using Eqs. (A1)–(A4).

In Fig. 5, we have plotted $(m^*/m_0)^2 = m_r^2$ versus $\Delta(1/H)^{-1}$ for six samples, following Eq. (A4), where the solid curve is a least-squares fit of the data to Eq. (A4). We determine the band-edge mass m_r^0 from the intercept and the matrix element $E_p = (2m_0/\hbar^2)P^2$ from the slope. We find $m_r^0 = 5.60 \pm 0.25 \times 10^{-3}$ and $E_p = 17 \pm 1.4$ eV. Since $m_r^0 = \frac{3}{2}(E_g/E_p)$, we find the interaction energy gap at $k = 0$ to be $E_g = 0.0635 \pm 0.008$ eV. Comparing this with E_g^p, we see that $E_g \simeq E_g^p - E_F$. Our value of E_p may be compared to 18 ± 1 eV ($Hg_{0.90}Cd_{0.10}Te$, HgTe)[4,18] and to 19 eV,[8] estimated from the difference between HgTe and a value of 21 eV for CdTe.[19] This latter is based on early mass measurements in CdS, CdSe, and CdTe and is supposed to represent the II-VI compounds. We may note here that recent HgSe data[20] give $E_p = 14.5 \pm 0.7$ eV. Clearly, one cannot yet establish a systematic variation in E_p across the $Hg_{1-x}Cd_xTe$ system. The present results, where a definite attempt has been made to eliminate uncertainties in some of the materials's parameters, give essentially the same matrix element as in HgTe.[18]

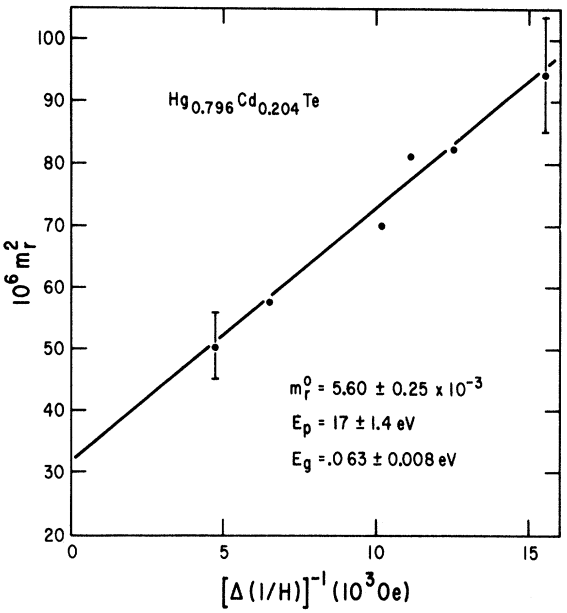

FIG. 5. Variation of the effective mass ratio $m^*/m_0 = m_r$ with the reciprocal of the Shubnikov–de Haas period, which is proportional to the Fermi-surface cross section. The solid curve is a least-squares fit of the data to Eq. (A4). The error bars represent the ±5% error in the experimental determination of all m_r.

For an energy band described by Kane's two-band model, the energy levels of an electron in an extremal orbit in a magnetic field, including electron spin, are given by

$$E_n(1 + E_n/E_g) = (n + \tfrac{1}{2})\hbar\omega_c \pm \tfrac{1}{2}g\mu H, \quad n = 0, 1, 2, \cdots \tag{1a}$$

where $\omega_c = eH/m^*c$, g is the electron g value, and μ is the Bohr magneton. Introducing a parameter $\delta = \frac{1}{2}gm^*/m_0$, we have

$$E_n(1 + E_n/E_g) = (n + \tfrac{1}{2} \pm \tfrac{1}{2}\delta)\hbar\omega_c, \tag{1b}$$

from which it may be seen that δ is the ratio of spin to Landau-level splitting. Spin splitting of the magnetoresistance extrema may be resolved as the lower quantum number levels pass the Fermi level and typical effects are shown in Fig. 2. The experimental value of δ is denoted by δ_{expt} defined by

$$\delta_{expt} = \frac{(H_N^+)^{-1} - (H_N^-)^{-1}}{\Delta(1/H)},$$

where H_N^+ and H_N^- are the magnetic field positions of the split peaks. However, the relation between δ_{expt} and g may be complicated by several factors. To make a positive identification of spin splitting, one must first eliminate effects which could introduce spurious structure in the oscillatory data. Such an effect is carrier-concentration inhomogeneity, which we find may lead to ambiguity, especially when the carrier concentration is sufficiently small to preclude definite beat patterns. This has been observed also in HgTe epitaxial films.[21] We studied numerous samples with essentially identical electron densities, reasoning that spin effects would give reproducible splittings while inhomogeneity would be random from sample to sample. We are confident that a real spin splitting of the $N = 1$, 2, and 3 Landau levels has been observed. Experimentally, we find that the structure is always more clearly resolved at higher magnetic fields. We must also consider the effects on δ_{expt} due to the magnetic-field–induced shift in the Fermi energy,[22] which can become significant at low quantum numbers. In addition, the inclusion of higher and lower bands will modify Eq. (1) such that the quantity gm^*/m_0 will depend on N.[23] These effects will be discussed presently.

We determined the splitting generally from the derivative extrema, but in a few cases confirmed that the magnitude of δ_{expt} was in satisfactory

agreement with that determined from the monotonic magnetoresistance. No angular dependence (± 3%) was detected in the spin splitting. It was found that δ_{expt} for the $N=1$ structure was generally about 25% greater than δ_{expt} ($N=2$) and about 30% larger than δ_{expt} ($N=3$). This effect has also been reported for InSb.[24] For $N=1$, we measure $\delta_{expt} = 0.46 \pm 0.02$ for all samples (Table I), and using this value, we have calculated the expected shift in Fermi energy with magnetic field. We find that the measured splittings will be larger by 5, 3, and 2% on the $N=1$, 2, and 3 levels, respectively,[25] than if the Fermi level were constant. Therefore, the large change in δ_{expt} reported above cannot be explained by this mechanism. Although we cannot calculate at the present time the influence of higher and lower bands on the quantity gm^*/m_0, the effect should be small. We therefore, tentatively ascribe the observed increase in δ_{expt} with N to the progressively improved resolution[23] and the preferred value is δ_{expt} ($N=1$). Correcting for the Fermi-level shift, we have $\delta = 0.96\ \delta_{expt} = 0.44$. At the band edge, $m^*/m_0 = 5.60\times10^{-3}$ so that $g_0 = 164$.

The energy dependence of g (ignoring higher-order bands) is given by[26]

$$g(k) = 2\left[1 - \left(\frac{m_0}{m^*} - 1\right)\frac{2\Delta}{3(E_F+E_g)+2\Delta}\right], \qquad (2)$$

where Δ is the spin-orbit splitting. Since $m_0/m^* \gg 1$, this is well approximated by

$$g(k)\frac{m^*(k)}{m_0} = \frac{2\Delta}{3(E_F+E_g)+2\Delta} = 2\delta\ . \qquad (2')$$

The magnitude of $\Delta \approx 1$ eV for HgTe and is probably not too different in the alloy, so the above formula predicts only a 3% increase in δ as the carrier concentration increases from 2×10^{15} to 1×10^{16} cm^{-3}. Thus, to our experimental accuracy, Eq. (2) predicts no energy dependence in δ, in agreement with the results. From our value of $\delta = 0.44$, Eq. (2) may be used to determine the spin-orbit splitting, and we find $\Delta = 0.75$ eV.

Using the measured value of g, we may now confirm the interpretation of the structure in the transverse magnetoresistance given earlier (Fig. 4). The magnetic field H_0^+ of the zeroth maximum in the transverse conductivity $\sigma_{xx} = \rho_{xx}(\rho_{xx}^2+\rho_{xy}^2)^{-1}$ is given by[15]

$$H_0^+ = n^{2/3}\frac{\hbar c}{e}(\sqrt{2}\pi^2)^{2/3}\left(\frac{g}{2}\frac{m^*}{m_0}\right)^{-1/3}. \qquad (3)$$

We have measured ρ_{xy} for two of the lightly doped alloys; on calculating σ_{xx} we find that the magnetic field for the σ_{xx} maximum is 6% lower than that for ρ_{xx}. As an example of the agreement between experiment and theory, for H_0^+ we find for Q190-15 that $H_0^+ = 13.4$ kOe, while the field calculated from Eq. (3) is $H_0^+ = 14.9$ kOe. The discrepancy may be due to Landau-level broadening, but an exact correction is not available. However, the agreement is sufficient to confirm the mechanism responsible for the observed structure in the transverse magnetoresistance.

ACKNOWLEDGMENTS

We are indebted to R. A. Reynolds, M. J. Brau, and H. Kraus for providing us with these alloys. Without their contribution, this work would not have been possible. It is a pleasure to acknowledge helpful discussions with R. T. Bate and D. D. Buss. Technical assistance was given by D. W. Attaway.

APPENDIX

The $\vec{k}\cdot\vec{p}$ theory has been adequately treated in the literature[7,27]; we merely summarize here several useful formulas applicable to our investigation.[8]

The Γ_6 conduction of $Hg_{0.796}Cd_{0.204}Te$ should be well described by the $\vec{k}\cdot\vec{p}$ dispersion relation valid for large spin-orbit splitting since $\Delta = 0.75$ eV:

$$E_c = \hbar^2k^2/2m_0 + \tfrac{1}{2}\left[E_g + (E_g^2 + \tfrac{8}{3}P^2k^2)^{1/2}\right], \qquad (A1)$$

where E_g is the energy gap, P is the momentum matrix element, and the energy is measured from the Γ_8 band edge. Near the Γ_6 minimum, the parameters a, b, and c, describing higher and lower bands,[7] have values $a \approx 1$, $b = c \approx 0$. The interaction between Γ_6 and the next higher conduction band Γ_{15} should be very small since $\Gamma_{15} - \Gamma_6 \gg 1$ eV, so that Eq. (A1) should be a good approximation to the real dispersion relation. Since the electron effective mass $m^* = \hbar^2k(dE/dk)^{-1}$, we have

$$m^*/m_0 = \left[1 + (4P^2/3\hbar^2)m_0(E_g^2 + \tfrac{8}{3}P^2k^2)^{-1/2}\right]^{-1}. \qquad (A2)$$

Writing $m^*/m_0 = m_r$, and $E_p = (2m_0/\hbar^2)P^2$, we have from (A1) and (A2)

$$\left(\frac{m_r}{1-m_r}\right) = \left(\frac{m_r^0}{1-m_r^0}\right)^2 + \frac{3\hbar^2}{m_0E_p}k^2, \qquad (A3)$$

where m_r^0 is the band-edge mass ratio given by

$$m_r^0 = \left(1 + \frac{2}{3}\frac{2m_0}{\hbar^2}\frac{P^2}{E_g}\right)^{-1}.$$

For a spherical surface, (A3) can be written

$$\left(\frac{m_r}{1-m_r}\right)^2 = \left(\frac{m_r^0}{1-m_r^0}\right)^2 + \frac{6e\hbar}{m_0cE_p}f$$

$$= \left(\frac{m_r^0}{1-m_r^0}\right)^2 + 6.90\times10^{-8}\frac{f}{E_p}, \qquad (A4)$$

where $f = [\Delta(1/H)]^{-1}$ is in Oe and E_p is in eV. The

quantity f is related to the extremal Fermi-surface cross section S through the relation $f=\hbar cs/2\pi e$. For $Hg_{0.796}Cd_{0.204}Te$, the electron mass ratio $m_r \ll 1$ (Sec. III), so the mass terms are well approximated by m_r^2 and $(m_r^0)^2$.

[1]T. C. Harman, W. H. Kleiner, A. J. Strauss, G. B. Wright, J. G. Mavroides, J. M. Honig, and D. H. Dickey, Solid State Commun. 2, 305 (1964).

[2]For example, C. Verie, in *Proceedings of the International Conference on II-VI Semiconducting Compounds, Providence, Rhode Island*, 1967, edited by D. G. Thomas (Benjamin, New York, 1968), p. 1124.

[3]R. A. Reynolds, C. G. Roberts, R. A. Chapman, and H. B. Bebb, in Proceedings of the International Conference on Photoconductivity, Stanford, 1969 (unpublished).

[4]T. C. Harman, in *Physics and Chemistry of II-VI Compounds*, edited by M. Aven and J. S. Prener (Wiley, New York, 1967), Chap. 15, Ref. 2, p. 982.

[5]W. Giriat, in Ref. 2, p. 1058.

[6]L. Sosnowski and R. R. Galazka, Ref. 5, p. 888.

[7]E. O. Kane, J. Phys. Chem. Solids 1, 249 (1957).

[8]J. D. Wiley and R. N. Dexter, Phys. Rev. 181, 1181 (1969).

[9]K. T. Aust, in *The Art and Science of Growing Crystals*, edited by J. J. Gilman (Wiley, New York, 1963), pp. 452-478.

[10]R. T. Bate and N. G. Einspruch, Phys. Rev. 153, 796 (1967).

[11]E. N. Adams and T. D. Holstein, J. Phys. Chem. Solids 10, 254 (1959).

[12]P. W. Kruse, D. Long, and O. N. Tufte, in Proceedings of the International Conference on Photoconductivity, Stanford, 1969 (unpublished).

[13]M. W. Scott, J. Appl. Phys. 40, 4077 (1969).

[14]R. L. Bell and K. T. Rogers, Phys. Rev. 152, 746 (1966).

[15]R. I. Bashirov, R. M. Gadzhieva, and E. M. Khanzhina, Fiz. i Tekhn. Poluprovodnikov 2, 1013 (1967) [Soviet Phys. Semicond. 2, 840 (1969)].

[16]A. L. Efros, Fiz. Tverd. Tela 7, 1501 (1965) [Soviet Phys. Solid State 7, 1206 (1965)].

[17]R. T. Bate, in *Semiconductors and Semimetals*, edited by R. K. Willardson and A. C. Beer (Academic, New York, 1968), Vol. 4, p. 459.

[18]S. H. Groves, R. N. Brown, and C. R. Pidgeon, Phys. Rev. 161, 779 (1967).

[19]M. Cardona, J. Phys. Chem. Solids 24, 1543 (1963).

[20]C. R. Whitsett, Phys. Rev. 138, A828 (1965).

[21]G. A. Antcliffe and H. Kraus, J. Phys. Chem. Solids 30, 243 (1969).

[22]G. Landwehr, in *Physics of Solids in Intense Magnetic Fields*, edited by E. D. Haidemenakis (Plenum, New York, 1969), p. 415.

[23]R. T. Bate (private communication).

[24]G. A. Antcliffe and R. A. Stradling, Phys. Letters 20, 119 (1966).

[25]D. D. Buss (private communication).

[26]W. Zawadski, Phys. Letters 4, 190 (1963).

[27]E. O. Kane, in *Semiconductors and Semimetals*, edited by R. K. Willardson and A. C. Beer (Academic, New York, 1966), Vol. 1, p. 75.